NUCLEAR INSTRUMENTS AND METHODS 65 (1968) 353–357; © NORTH-HOLLAND PUBLISHING CO.

MEASUREMENT OF THE LIMIT OF SENSITIVITY OF HYDROGEN IN A BUBBLE CHAMBER AND CALIBRATION OF PRESSURE GAUGES

G. HORLITZ and S. WOLFF

Deutsches Elektronen-Synchrotron DESY, Hamburg

and

G. HARIGEL

CERN, Geneva, Switzerland

Received 10 June 1968

A new method of calibrating pressure gauges in bubble chambers under operating conditions is described.

Starting with different static pressures p_s, greater than the vapour pressure p_v, the dynamic pressure in a bubble chamber is reduced to an arbitrary, fixed value $p(b,T)$. At a given temperature T, the appearance of this pressure is indicated by a constant bubble density b. A plot of the signal U of a pressure transducer [corresponding to the pressure drop p_s-$p(b,T)$] against the static pressure p_s, gives a straight line for every single $b = \text{const}$. The slope of these lines is equal to the sensitivity of the gauge. The extrapolated experimental line intersects the axis $U = 0$ in the point $p_s = p(b,T)$, which is independent of the calibration factor of the transducer.

In a 85 cm bubble chamber, $p(b,T)$ has been measured in the temperature interval $24.5 < T < 28.0°\text{K}$ with $b = 0$, which represents the limit of sensitivity in a p-T diagram for relativistic electrons.

1. Introduction

The knowledge of operating conditions of bubble chambers becomes more and more important, both from theoretical and practical points of view. One of the most critical parameters is the dynamic pressure in the bubble chamber. Up to now, different pressure gauges, such as strain gauges, capacitive and inductive devices have been used.

Disagreements of pressure dependent experimental results of different bubble chambers may be explained by errors in the calibration methods of these pressure indicators.

In the 85 cm hydrogen bubble chamber operated at DESY, commercially available piezo-electric quartz transducers are used since two years. Their calibration is described in the following sections.

2. Theoretical considerations

Starting from a static pressure p_s, the pressure in the bubble chamber liquid is reduced to a value $p_s - \Delta p$ (fig. 1). An electronic measuring device (in our case a quartz gauge with charge amplifier) gives an electrical voltage signal, which is proportional to this pressure drop:

$$U = a \cdot \Delta p. \tag{1}$$

The bubble chamber is expanded to a certain value of pressure $p(b,T)$, which at a given temperature T is associated with a certain bubble density b.

For a given $p_s = p_{s_1}$, we find (fig. 1),

$$\Delta p_1 = p_{s_1} - p(b,T) \tag{2}$$

and

$$U_1 = a[p_{s_1} - p(b,T)]. \tag{3}$$

If we change the static pressure from p_{s_1} to p_{s_2}, we also have a change Δp in order to get the same bubble density b. This results in another signal of the transducer.

$$U_2 = a[p_{s_2} - p(b,T)]. \tag{3a}$$

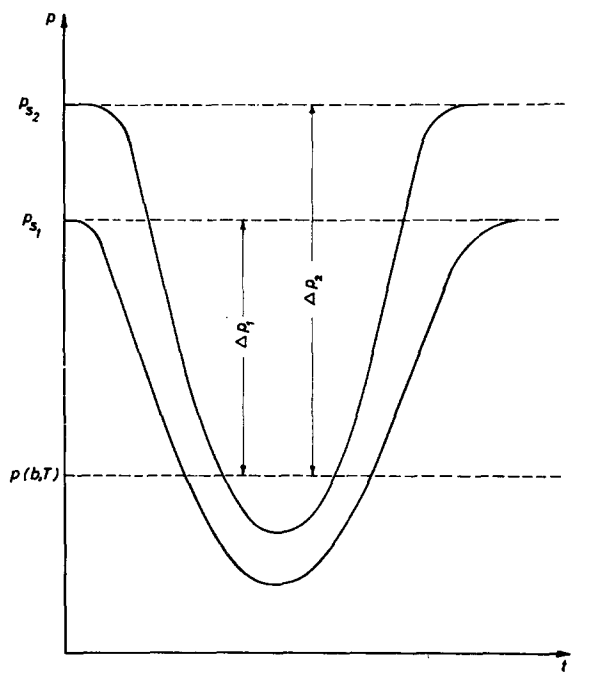

Fig. 1. Pressure vs time curves (schematic).

One can use the bubble density b as an indicator for the pressure, provided that in a given liquid for particles of equal mass and momentum, b depends only on the temperature of the liquid and on the instantaneous pressure at the moment of the passage of the particle (an assumption which is in accordance with theory[1-4]).

From

$$b(p,T) = \text{const. at } T = \text{const.},$$

follows

$$p(b,T) = \text{const. at } T = \text{const.} \tag{4}$$

A plot of the voltage U as a function of the static pressure p_s

$$U(b,p_s,T) = a[p_s - p(b,T)] \tag{5}$$

gives, under the conditions of eq. (4), a straight line for each $b = \text{const.}$

As long as $T = \text{const.}$, the slope of these lines

$$a^* = \mathrm{d}U/\mathrm{d}p_s, \tag{6}$$

is identical with the calibration factor a.

However, the conditions of eq. (4) can experimentally be realized only in the case of an isothermal expansion. Practically all bubble chamber expansions are so fast that they have to be considered as being adiabatic. The consequence of this adiabatic pressure reduction is a temperature drop

$$\Delta T = \int_{p_s}^{p(b,T)} (\mathrm{d}T/\mathrm{d}p)\mathrm{d}p. \tag{7}$$

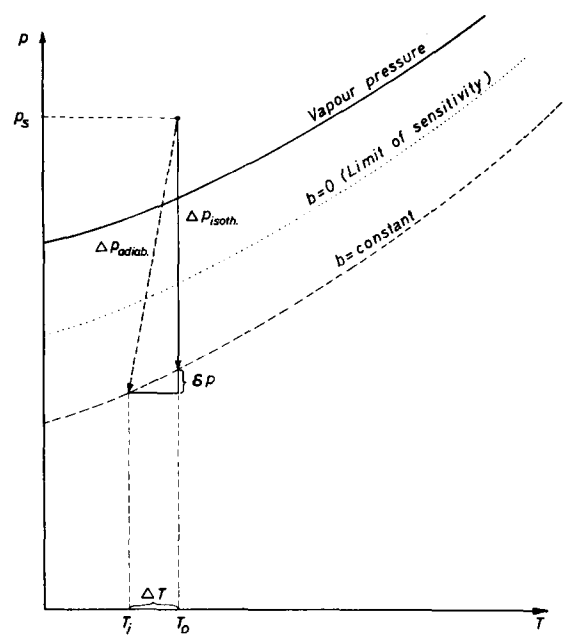

Fig. 2. p-T diagram with $p(b,T)$ curves (schematic).

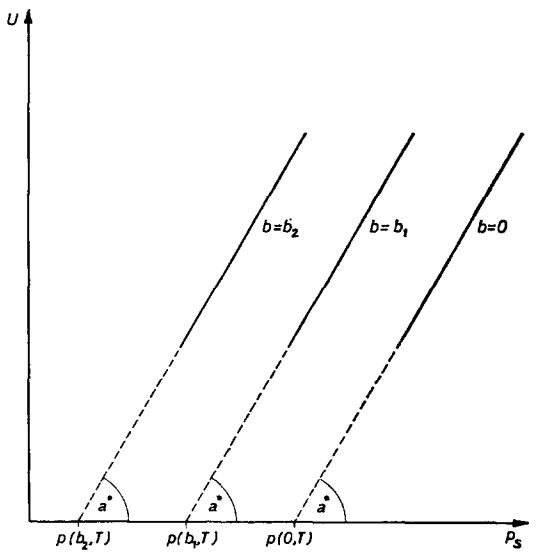

Fig. 3. $U = f(p_s)$ for different bubble densities b and $T = \text{const.}$ (schematic).

The adiabatic temperature change $\mathrm{d}T/\mathrm{d}p$ can be calculated from the theory of thermodynamics

$$(\mathrm{d}T/\mathrm{d}p)_{\text{adiab.}} = (1/\alpha)(\beta - \beta'), \tag{8a}$$

or

$$(\mathrm{d}T/\mathrm{d}p)_{\text{adiab.}} = (\beta/\alpha)\{1 - (1/\gamma)\}, \tag{8b}$$

with

$\alpha = V^{-1}(\partial V/\partial T)_p$: factor of thermal expansion,

$\beta = -V^{-1}(\partial V/\partial p)_T$: isothermal compressibility,

$\beta' = -V^{-1}(\mathrm{d}V/\mathrm{d}p)_{\text{adiab.}}$: adiabatic compressibility.

β and β' are correlated by

$$\beta' = \beta/\gamma, \tag{9}$$

$\gamma = c_p/c_v$: ratio of specific heats.

In a p-T diagram (fig. 2) this influence of ΔT is shown. For obtaining the desired bubble density b at a lower temperature $T_i = T_0 - \Delta T$, one has to reduce the pressure by an additional amount δp. If the curves of constant bubble density $p(b,T)$ are known, one can calculate

$$\delta p = \{\partial p(b,T)/\partial T\}\Delta T \tag{10}$$

and

$$p(b,T) = p(b,T_0) + \{\partial p(b,T)/\partial T\}\Delta T. \tag{11}$$

ΔT can be calculated from eq. (7). If one neglects, in a first approximation, the pressure dependence of $\mathrm{d}T/\mathrm{d}p$ within the operating limits of p one gets

$$\Delta T = -(\mathrm{d}T/\mathrm{d}p)[p_s - p(b,T)] \quad (12)$$

and with eq. (11)

$$p(b,T) = [p(b,T_0) - p_s\{\partial p(b,T)/\partial T\}(\mathrm{d}T/\mathrm{d}p)]\cdot \cdot[1 - \{\partial p(b,T)/\partial T\}(\mathrm{d}T/\mathrm{d}p)]^{-1}. \quad (13)$$

Inserting eq. (13) into eq. (5) for the transducer signal, we get finally

$$U = a\{p_s - p(b,T_0)\}[1 - \{\partial p(b,T)/\partial T\}(\mathrm{d}T/\mathrm{d}p)]^{-1}, \quad (14)$$

$$U = a^*[p_s - p(b,T_0)], \quad (15)$$

with

$$a^* = \mathrm{d}U/\mathrm{d}p_s = a[1 - \{\partial p(b,T)/\partial T\}(\mathrm{d}T/\mathrm{d}p)]^{-1}. \quad (16)$$

From eqs. (14), (15) and (16) one can see that in a plot $U = f(p_s)$, $b = \text{const.}$, we get straight parallel lines as in the case of $T = \text{const.}$, but now with a slope $a^* \neq a$.

Using eq. (16) one calculates

$$a = a^*[1 - \{\partial p(b,T)/\partial T\}(\mathrm{d}T/\mathrm{d}p)]. \quad (17)$$

An extrapolation of the lines $U = f(p_s)$ to $U = 0$ intersects the p_s-axis in $p_s = p(b,T_0)$; (fig. 3).

This gives a new method to measure the curves of constant bubble density $p(b,T)$ in the p-T diagram. Knowledge of the calibration factor of the dynamic pressure measuring device is not necessary for this purpose. It will be sufficient if the overall response of the measuring system is linear.

3. Experimental arrangement

The first measurements in the DESY 85 cm hydrogen bubble chamber were limited to the special case $b = 0$. The main purpose was, to determine the calibration factor of the quartz gauge and to test the method. The experimental set-up is shown in fig. 4.

The bubble chamber was exposed to an electron beam with a momentum of about 2 GeV/c and a pulse length of about 5 μs. The injection time of the electrons was indicated by a trigger pulse from a scintillation counter. This pulse was delayed; it fired the flashtubes of the illumination system 2 ms after the injection of the beam, so as to allow the bubbles to grow to a visible size. The bubble tracks have been observed in natural size on the monitor screen of a television camera[5]).

The amplified signal of the pressure transducer was displayed on one of the inputs of a dual trace oscilloscope; the second input was used to mark the beam arrival by means of the pulse of a scintillation counter placed in the beam. The start of the expansion system was shifted with respect to the beam arrival until the tracks appeared or disappeared on the monitor screen. The voltage signal U, which corresponds to the instantaneous pressure at the moment of beam injection, was measured with an accuracy of 1%, using a compensating amplifier. The pressure at which bubbles appeared, was reproducible within less than ± 0.1 kg/cm^2.

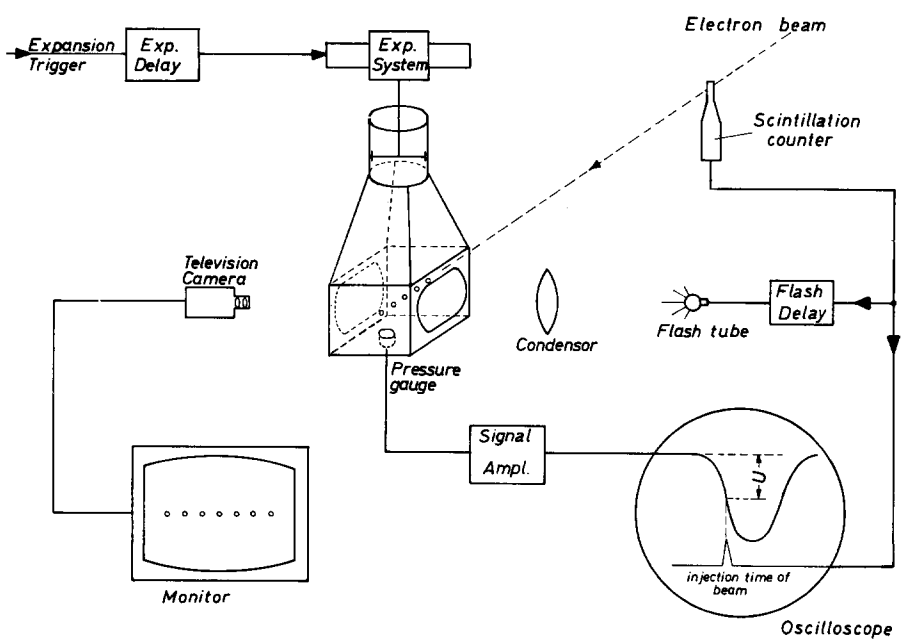

Fig. 4. Experimental arrangement.

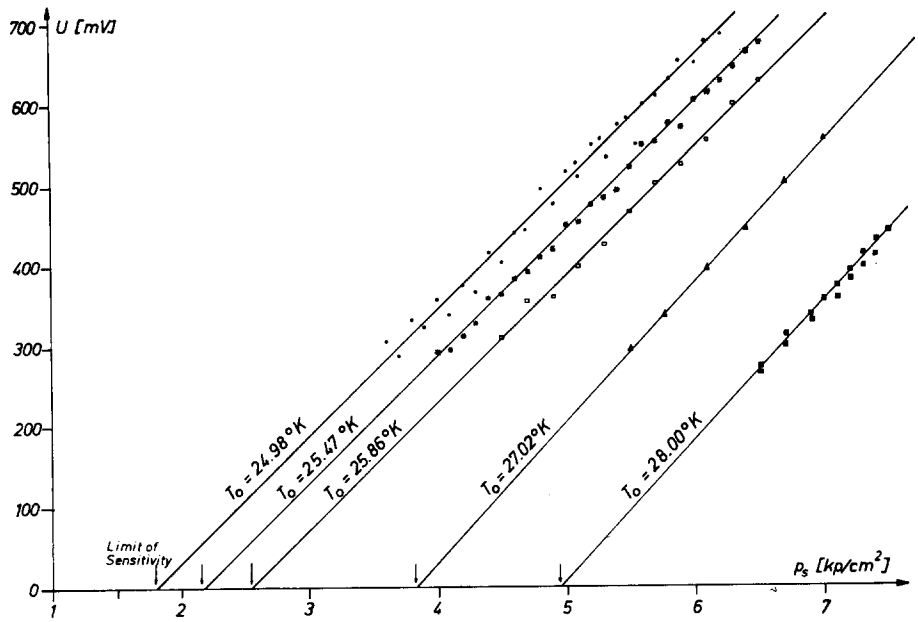

Fig. 5. Calibration of quartz pressure gauge at different temperatures.

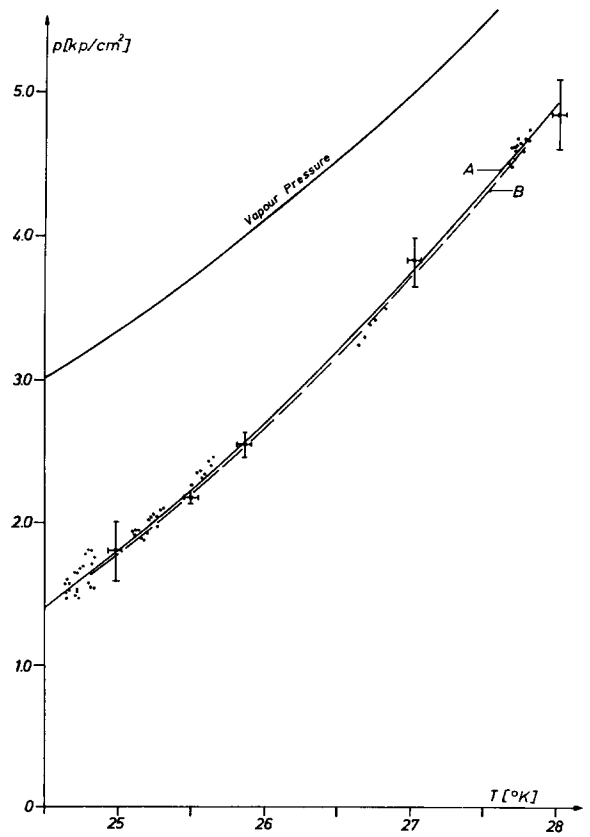

Fig. 6. Limit of sensitivity in liquid H_2. a. From pressure gauge calibration curves; b. From bubble counting.

4. Experimental results

Fig. 5 represents the measurements $U = f(p_s)$ in hydrogen between 25.0 and 28.0° K.

From these curves we take the slope a^* and the limit of sensitivity $p(b,T_0)_{b=0}$ (curve A in fig. 6).

Using $\partial p(b,T)/\partial T$ from this diagram and eq. (17) we get the calibration factor a. The data used for these calculations as well as the results are given in the table 1.

The mean value of a for the applied quartz gauge (type Kistler 410 A with charge amplifier type Kistler 566 set to a nominal sensitivity of 1 mV/pC) is

$$a = 147 \pm 7 \qquad [\mathrm{mV}/(\mathrm{kg/cm^2})].$$

With a and $\mathrm{d}T/\mathrm{d}p$ known, from eq. (8a), we are able to calculate for each single measuring point of fig. 5 the pressure and temperatures related to the limit of sensitivity. Fig. 6 shows that all these points are very well represented by curve A. This is a good check for the consistency of the method.

The results of bubble density measurements, which have been evaluated by bubble counting on films[8]), are also indicated in this figure (curve B). The agreement of the results found by these two methods is very satisfying.

We are greatly indebted to Professor M. W. Teucher and Dr. E. Lohrmann for their continued interest and encouragement in the course of these investigations. We also thank our bubble chamber team, especially

TABLE 1
Thermodynamical parameters.

T_0 [°K]	$\alpha \times 10^2$ [°K]$^{-1}$	$\beta \times 10^3$ [kg/cm^2]$^{-1}$	$\beta' \times 10^3$ [kg/cm^2]$^{-1}$	a^* [mV/(kg/cm^2)]	$dp(b=0;T_0)/dT$ [(kg/cm^2)/°K]	dT/dp [°K/(kg/cm^2)]	a [mV/(kg/cm^2)]
24.98	2.70	3.77	1.69	156.7	1.0	0.077	144.4
25.47	2.89	4.16	1.81	155.9	1.0	0.081	143.0
25.86	3.05	4.48	1.88	156.8	1.0	0.085	143.2
27.02	3.54	5.55	1.92	173.5	1.06	0.103	155.2
28.00	4.24	7.07	2.16	171.9	1.12	0.116	149.7
Ref.	[6]	[6]	[7]				

W. Eschricht, H. J. Fiebig, U. Knopf, K. D. Nowakowski, O. Peters and W. Stahlschmidt.

Furthermore we have to thank the DESY machine group as well as H. Meyer and the beam operating crew for the excellent performance of the synchrotron and the beam.

References

[1] F. Seitz, Physics of Fluids **1** (1958) 2.
[2] A. G. Tenner, Nucl. Instr. and Meth. **22** (1963) 1.
[3] B. N. Fabian, R. L. Place, W. A. Riley, W. H. Sims and V. P. Kenney, Rev. Sci. Instr. **34** (1963) 484.
[4] P. Kunkel, Dissertation (Würzburg, 1967).
[5] Erfahrungen bei der Verwendung einer Fernsehkamera zur Beobachtung von Blasenkammer-Spuren. DESY-B1 (1966) Int. Report, unpublished.
[6] A. D. Little, *Hydrogen Handbook* (Cambridge, 1960).
[7] G. Horlitz, S. Wolff and G. Harigel, On the thermodynamics of bubble chamber expansions (to be published).
[8] G. Harigel, G. Horlitz and S. Wolff. Measurements of bubble densities in liquid hydrogen and liquid deuterium (to be published).